Conformational Behaviour of Medium-sized Rings. Part II.[1] Heterocyclic Analogues of 5,6,7,12-Tetrahydrodibenzo[*a,d*]cyclo-octene (1,2,4,5-Dibenzocyclo-octa-1,4-diene)†

By **Robert P. Gellatly, W. David Ollis,*** and **Ian O.Sutherland,** Department of Chemistry, The University, Sheffield S3 7HF

The temperature dependence of the n.m.r. spectra of a number of heterocyclic analogues (2) of 5.6,7,12-tetrahydrodibenzo[*a,d*]cyclo-octene has been interpreted in terms of the interconversion of chair- and boat-like conformations. These interpretations have been supported by strain energy calculations, and there is a useful correlation between the activation parameters determined by variable temperature n.m.r. spectroscopy and the results provided by these calculations. The 12-oxodibenz[*c,f*]azocine derivative (2l) apparently exists preferentially in a boat conformation as a consequence of a weakly bonding interaction between N(6) and the C(12) carbonyl function.

In Part I [1] we discussed the conformational behaviour of 5,6,11,12-tetrahydrodibenzo[*a,e*]cyclo-octene (1) and some heterocyclic analogues. These compounds showed temperature dependence of their n.m.r. spectra which could be associated with chair- and boat-like conformations undergoing inversion and interconversion at relatively low rates on the n.m.r. time scale. Since this work was completed a number of papers have appeared concerning conformational studies of the hydrocarbon (1),[2] some heterocyclic analogues of (1),[3] the related hydrocarbon *cis,cis*-1,5-cyclo-octadiene,[4] and its *syn*-3,7-dibromo derivative.[5] It is clear from these results that the 1,5-cyclo-octadiene system can show interesting conformational behaviour involving a rigid chair conformation and a mobile boat conformation.[6] It is evident from the examination of models and from geometrical considerations [6] that the 1,4-cyclo-octadiene system might show similar conformational behaviour. We have therefore examined some heterocyclic analogues (2) of 5,6,7,12-tetrahydrodibenzo[*a,d*]cyclo-octene using n.m.r. line-shape methods [7] which have been demonstrated to be a powerful technique for solving the subtle problems posed by the conformational behaviour of cyclic compounds in solution.

The cyclic sulphides (2a),[8] (2d), (2g), and (2i) were prepared by the reaction of the corresponding bis(bromomethyl) compounds (3a—d) with sodium sulphide. Bis-(2-bromomethylphenyl)methane (3a) was prepared by a published procedure,[9] with slight variations as noted in the Experimental section. The bis(bromomethylphenyl) ether (3b) and sulphide (3c) were prepared by controlled side-chain bromination of the corresponding di-*o*-tolyl derivatives. The sulphones (2b),[8] (2l), (2j), and (3d) were readily prepared by oxidation of the corresponding sulphides with peracetic acid. The amines (2c), (2f), (2h), and (2k) were prepared by the reaction of the corresponding bis(bromomethyl) compound (3) with benzylamine in benzene. The compounds (2a—k) were formulated as shown on the basis of the synthetic procedures used, their molecular formulae (analysis and molecular weight or high resolution molecular weight), and their spectral characteristics (Experimental section and Table 1).

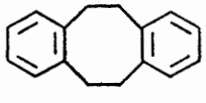

(1)

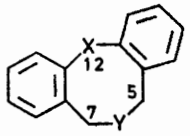

(2)

a; X = CH_2, Y = S
b; X = CH_2, Y = SO_2
c; X = CH_2, Y = N·CH_2Ph
d; X = O, Y = S
e; X = O, Y = SO_2
f; X = O, Y = N·CH_2Ph
g; X = Y = S
h; X = S, Y = N·CH_2Ph
i; X = SO_2, Y = S
j; X = Y = SO_2
k; X = SO_2, Y = N·CH_2Ph
l; X = CO, Y = N·CH_2Ph
m; X = CH_2, Y = NMe
n; X = CH_2, Y = N·CMe_3

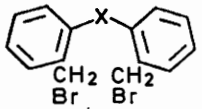

(3)

a; X = CH_2
b; X = O
c; X = S
d; X = SO_2
e; X = CO

6-Benzyl-6,7-dihydrodibenz[*c,f*]azocin-12(5*H*)-one (2l) was prepared in rather low overall yield from 2,2′-dimethylbenzophenone by bromination to give the bis(bromomethyl) ketone (3e) [10] which reacted with benzylamine to give the amine (2l). The azocine structure (2l) for this product is consistent with the molecular formula (analysis and molecular weight) and its spectral characteristics.

EXPERIMENTAL

Unless otherwise stated i.r. spectra were determined for dispersions in KBr using a Perkin-Elmer 137 spectrometer

† Throughout this paper we have used the nomenclature recommended by I.U.P.A.C. rule A-21.4, as in Part I.

[1] Part I, R. Crossley, A. P. Downing, M. Nógrádi, A. Braga de Oliveira, W. D. Ollis, and I. O. Sutherland, *J.C.S. Perkin I*, 1973, 205.

[2] D. Montecalvo, M. St. Jacques, and R. Wasylishen, *J. Amer. Chem. Soc.*, 1973, **95**, 2023.

[3] A. Saunders and J. M. Sprake, *J.C.S. Perkin II*, 1972, 1660.

[4] F. A. L. Anet and L. Kozerski, *J. Amer. Chem. Soc.*, 1973, **95**, 3407.

[5] R. K. Mackenzie, D. D. MacNicol, H. H. Mills, R. A. Raphael, F. B. Wilson, and J. A. Zabkiewicz, *J.C.S. Perkin II*, 1972, 1632.

[6] J. D. Dunitz and J. Waser, *J. Amer. Chem. Soc.*, 1972, **94**, 5645.

[7] For reviews, see G. Binsch, *Topics Stereochem.*, 1968, **3**, 97; I. O. Sutherland, *Ann. Reports N.M.R. Spectroscopy*, 1971, **4**, 71.

[8] D. D. Emrick and W. E. Truce, *J. Org. Chem.*, 1961, **26**, 1329.

[9] E. D. Bergmann and Z. Pelchowicz, *J. Amer. Chem. Soc.*, 1953, **75**, 4281.

[10] M. P. Cava and J. A. Kuczkowski, *J. Amer. Chem. Soc.*, 1970, **92**, 5800.

and u.v. spectra for ethanolic solutions using a Perkin-Elmer 137 UV spectrometer. N.m.r. spectra were measured for solutions in deuteriochloroform using a Varian HA-100 spectrometer. Low resolution mass spectra were determined with an A.E.I. MS12 spectrometer and high resolution spectra with an A.E.I. MS9 spectrometer. M.p.s were measured with a Reichert hot-stage apparatus. Microanalyses were determined by the University of Sheffield Microanalytical Service.

Preparative t.l.c. was carried out using Merck silica gel G. Solutions were dried over anhydrous magnesium sulphate and were evaporated under diminished pressure using a rotary evaporator.

Bis-(2-bromomethylphenyl)methane (3a).—The method of Bergmann and Pelchowicz [9] was used with the following modifications. (*a*) The methylation of 2,2′-methylenedibenzoic acid was carried out using diazomethane rather than sulphuric acid–methanol; and (*b*) the bromination of 2,2′-methylenedibenzyl alcohol was carried out using boiling hydrobromic acid for 20 min, cooling, and collecting the precipitated product. The diphenylmethane derivative (3a) had m.p. 92—93° (lit.,[9] 93—94°) (Found: C, 51.0; H, 3.9; Br, 45.25. Calc. for $C_{15}H_{14}Br_2$: C, 50.85; H, 4.0; Br, 45.2%).

7,12-*Dihydro*-5H-*dibenzo*[c,f]*thiocin* (2a).—The method of Emrick and Truce [8] was used; the product crystallised from benzene–ethanol (1 : 1); m.p. 193—194° (lit.,[8] 194.5°) (Found: C, 79.9; H, 6.2%; M^+, 226. Calc. for $C_{15}H_{14}S$: C, 79.6; H, 6.2%; *M*, 226).

7,12-*Dihydro*-5H-*dibenzo*[c,f]*thiocin* SS-*Dioxide* (2b).—The method of Emrick and Truce [8] was used; the product crystallised from benzene–toluene (4 : 1); m.p. 259—260° (lit.,[8] 258—259°) (Found: C, 69.7; H, 5.3; S, 12.55%; M^+, 258. Calc. for $C_{15}H_{14}O_2S$: C, 69.8; H, 5.4; S, 12.4%; *M*, 258).

6-*Benzyl*-5,6,7,12-*tetrahydrodibenz*[c,f]*azocine* (2c).—The method of Pala *et al.*[11] was used; the product crystallised from ethanol; m.p. 110—112° (lit.,[11] 113—114°) (Found: C, 88.1; H, 6.9; N, 4.8%; M^+, 299. Calc. for $C_{22}H_{21}N$: C, 88.3; H, 7.0; N, 4.7%; *M*, 299).

5H,7H-*Dibenz*[b,g][1,5]*oxathiocin* (2d).—A mixture of bis-(2-bromomethylphenyl) ether [12] (3b) (0.5 g) and sodium sulphide nonahydrate (1.5 g) in 95% aqueous methanol (80 ml) was heated under reflux with stirring for 46 h. The mixture was evaporated and the residual gum extracted with hot ethanol. The extract was cooled giving the *oxathiocin* (2d) (76 mg, 25%), m.p. 75—76° (Found: C, 73.6; H, 5.1; S, 14.1%; M^+, 228. $C_{14}H_{12}OS$ requires C, 73.7; H, 5.3; S, 14.0%; *M*, 228).

5H,7H-*Dibenz*[b,g][1,5]*oxathiocin* SS-*Dioxide* (2e).—A mixture of the oxathiocin (2d) (96 mg) and hydrogen peroxide (0.5 g; 30%) in acetic acid (1 ml) was heated under reflux for 1 h. The solution was allowed to cool and the precipitate collected giving the *sulphone* (2e), which crystallised from ethanol; yield 41 mg (37%), m.p. 152—154° (Found: C, 64.4; H, 4.4; S, 12.6%; M^+, 260. $C_{14}H_{12}O_3S$ requires C, 64.6; H, 4.6; S, 12.3%; *M*, 260); $\lambda_{max.}$ 220 nm (ε 24 800).

6-*Benzyl*-6,7-*dihydro*-5H-*dibenz*[b,g][1,5]*oxazocine* (2f).—A solution of benzylamine (0.9 g) in benzene (10 ml) was added dropwise over 30 min to a solution of bis-(2-bromomethylphenyl) ether (3b) (1.0 g) in boiling benzene (10 ml). Heating was continued for a further 2.5 h, then the mixture was cooled and filtered and the filtrate evaporated. The residual solid crystallised from ethanol giving the *oxazocine* (2f) (86 mg, 10%), m.p. 137—139° (Found: C, 83.8; H, 6.5; N, 4.65%; M^+, 301. $C_{21}H_{19}NO$ requires C, 83.7; H, 6.3; N, 4.65%; *M*, 301).

Bis-(2-bromomethylphenyl) Sulphide (3c).—A stirred mixture of di-*o*-tolyl sulphide [13] (12.5 g), *N*-bromosuccinimide (21.0 g), and dibenzoyl peroxide (0.1 g) in carbon tetrachloride (60 ml) was irradiated for 6 h with a tungsten lamp. The mixture was filtered, and the filtrate was evaporated giving a yellow gum which was repeatedly extracted with hot light petroleum (b.p. 40—60°). The extract was concentrated and cooled giving the *sulphide* (3c) (7.18 g, 33%), m.p. 68—70°. A sample recrystallised from light petroleum (b.p. 40—60°) had m.p. 69—70° (Found: C, 44.9; H, 3.45; Br, 42.9; S, 8.5. $C_{14}H_{12}Br_2S$ requires C, 45.2; H, 3.2; Br, 43.0; S, 8.6%); τ ($CDCl_3$) 5.25 (s, 2 × CH_2Br).

5H,7H-*Dibenzo*[b,g][1,5]*dithiocin* (2g).—A mixture of bis-(2-bromomethylphenyl) sulphide (3c) (0.5 g) and sodium sulphide nonahydrate (1.5 g) in 95% aqueous methanol (80 ml) was heated under reflux for 24 h with stirring. The mixture was evaporated and the residue distributed between benzene and water. The benzene layer was dried and evaporated. The residual solid crystallised from ethanol giving the *dithiocin* (2 g) (156 mg, 47%), m.p. 128—130° (Found: C, 68.7; H, 5.3; S, 26.6%; M^+, 244.0380. $C_{14}H_{12}S_2$ requires C, 68.9; H, 4.9; S, 26.2%; *M*, 244.0384).

6-*Benzyl*-6,7-*dihydro*-5H-*dibenzo*[b,g][1,5]*thiazocine* (2h).—A solution of benzylamine (0.47 g) in benzene (5 ml) was added dropwise over 1.5 h to a solution of bis-(2-bromomethylphenyl) sulphide (3c) (0.5 g) in boiling benzene (6 ml). After heating for a further 1 h, the mixture was filtered and the filtrate evaporated. The residue was purified by t.l.c. with benzene as solvent giving the *thiazocine* (2h) (76 mg, 18%), which crystallised from 95% ethanol; m.p. 91—92° (Found: M^+, 317.1249. $C_{21}H_{19}NS$ requires *M*, 317.1238).

Bis-(2-bromomethylphenyl) Sulphone (3d).—A mixture of bis-(2-bromomethylphenyl) sulphide (3c) (0.5 g) and hydrogen peroxide (1.14 g; 30%) in acetic acid (9 ml) was heated under reflux for 3 h. The mixture was evaporated and the residue purified by t.l.c. with benzene as solvent. The *sulphone* (3d) (106 mg, 20%) crystallised from ethanol; m.p. 128—131° (Found: C, 41.5; H, 3.1; Br, 39.6; S, 8.1%; M^+, 404. $C_{14}H_{12}Br_2O_2S$ requires C, 41.6; H, 3.0; Br, 39.6; S, 7.9%; *M*, 404).

5H,7H-*Dibenzo*[b,g][1,5]*dithiocin* 12,12-*Dioxide* (2i).—A mixture of bis-(2-bromomethylphenyl) sulphone (3d) (0.5 g) and sodium sulphide nonahydrate (1.38 g) in 95% methanol (80 ml) was heated under reflux with stirring for 40 h. The mixture was evaporated and the residue distributed between chloroform and water. The chloroform layer was dried and evaporated. The residual gum was purified by t.l.c. with chloroform as solvent, giving the *dithiocin* (2i), which crystallised from ethanol; m.p. 160—166° (134 mg, 39%) (Found: M^+, 276.0277. $C_{14}H_{12}O_2S_2$ requires *M*, 276.0279); $\lambda_{max.}$ 250 nm (ε 7 300).

5H,7H-*Dibenzo*[b,g][1,5]*dithiocin* 6,6,12,12-*Tetraoxide* (2j).—A mixture of the dithiocin dioxide (2i) (60 mg) and hydrogen peroxide (0.5 ml; 30%) in acetic acid (2 ml) was

[11] G. Pala, A. Montegani, and E. Zugna, *Tetrahedron*, 1970, **26**, 1275.

[12] R. Shapiro and D. Slobodin, *J. Org. Chem.*, 1969, **34**, 1165.

[13] M. Balasubramanian and V. Baliah, *J. Chem. Soc.*, 1955, 1251; F. Mauther, *Ber.*, 1906, **39**, 3593.

heated under reflux for 26 h. The mixture was cooled and the precipitate collected, giving the *disulphone* (2j), which crystallised from ethanol; yield 29 mg (38%), m.p. 293° (Found: C, 54.6; H, 4.05; S, 20.8%; M^+, 308. $C_{14}H_{12}O_4S_2$ requires C, 54.5; H, 3.9; S, 20.8%; *M*, 308); $\lambda_{max.}$ 220 (ε 18 300) and 262 nm (5 000).

6-*Benzyl*-6,7-*dihydro*-5H-*dibenzo*[b,g][1,5]*thiazocine* SS-*Dioxide* (2k).—A solution of benzylamine (0.44 g) in benzene (5 ml) was added dropwise over 2 h to a solution of bis-(2-bromomethylphenyl) sulphone (3d) (0.5 g) in boiling benzene (10 ml). After heating for a further 30 min, the mixture was filtered, and the filtrate evaporated giving a gum which was purified by t.l.c. with benzene as solvent. The *thiazocine dioxide* (2k) crystallised from benzene; yield 97 mg (22%), m.p. 164—166° (Found: M^+, 349.1141. $C_{21}H_{19}O_2NS$ requires *M*, 349.1137); $\lambda_{max.}$ 245 nm (ε 15 200).

6-*Benzyl*-6,7-*dihydrodibenz*[c,f]*azocin*-12(5H)-*one* (2l).—A mixture of 2,2′-dimethylbenzophenone [14] (0,5 g), *N*-bromosuccinimide (1.0 g), and dibenzoyl peroxide (0.01 g) in carbon tetrachloride (40 ml) was irradiated for 2 h at room temperature using a tungsten lamp. The mixture was filtered and the stirred filtrate treated dropwise at 0 °C with a solution of benzylamine (0.72 g) in carbon tetrachloride (5 ml). The mixture was then filtered, and the filtrate evaporated giving a gum (0.97 g) which was separated by t.l.c. with chloroform as solvent. The major component crystallised from benzene giving the *azocine* (21), m.p. 106—107° (29 mg, 4%) (Found: C, 84.4; H, 6.2; N, 4.3%; M^+, 313. $C_{22}H_{19}NO$ requires C, 84.35; H, 6.1; N, 4.5%; *M*, 313); $\lambda_{max.}$ 221 (ε 24 600) and 265 nm (1 300).

Determination of Exchange Rates by N.m.r. Spectroscopy.[7] —The methods used were fully described in Part I.[1] In general, exchange rates were determined at a single temperature only (Table 2) so that only free energies of activation could be calculated. The computer programs (coded in FORTRAN IV) used to generate theoretical line-shapes are described for four general methods (I—IV).

Method I. A program * was used that was suitable for the calculation of n.m.r. line-shapes for two AB systems (A1,B1 and A2,B2) undergoing exchange of hydrogen nuclei between the pairs of sites designated A2 and B2, A1 and A2, and B1 and B2. In all cases the exchange rate (k_2) between the sites A2 and B2 was fast compared with the exchange rates (k_{12} and k_{21}) between the sites A1 and A2 and B1 and B2.† Thus nuclei in the sites A2 and B2 give rise to a single line (AB2) at the average site chemical shift at temperatures where the sites A1 and B1 give rise to a typical four-line AB system [for an example see Figure 1(a)]. This situation was observed in the spectra of compounds (2d, f, and h) at low temperatures (down to −110 °C) and in the spectra of compounds (2e and g) at intermediate temperatures (*e.g.* −52 and +20 °C, respectively). In these cases the input parameters for spectrum simulation (chemical shifts, coupling constant, J_1, and population, p_1) for the system A1,B1 were readily obtained from the low temperature spectra, but for the system A2,B2 the only critical input parameters were the population (p_2) and average chemical shift provided that the exchange rate k_2 was large (*e.g.* $>10^4$ s^{-1}). The input relaxation times were based upon low temperature spectral line-widths in the usual way.[1,7] Agreement between observed and calculated spectral line-shapes could usually be obtained quite readily [*e.g.* Figure 1, (a) and (b)], but in two cases, compounds (2i and k), the population, p_2, of the sites A2 and B2 was so low that the singlet expected from these sites at temperatures where $k_2 \longrightarrow \infty$ but $k_{12} \longrightarrow 0$ could not be distinguished in the experimental spectra ($p_2 <$ *ca.* 0.05). In these two cases it was assumed that the average chemical shift for the sites A2 and B2 was that found for analogous compounds (see Table 1), and with $k_2 \longrightarrow \infty$ the populations p_1 and p_2 were adjusted to give a good match between observed and computed spectral line-shapes. In general the spectra observed for these two compounds, (2i and k), as k_{12} increased were similar to those of a single AB system based upon the sites A1 and B1, but

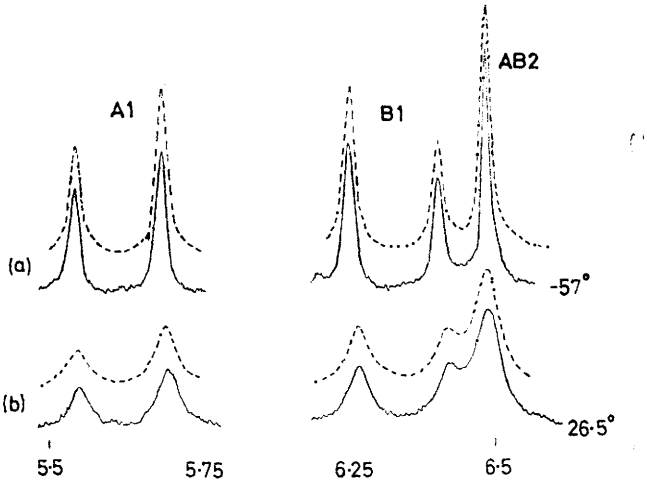

FIGURE 1 Observed (full line) and computed (broken line) spectra of the C-5 and C-7 methyene protons of the oxathiocin derivative (2d): (a) at −57° C, (b) at −26.5 °C; $k_{12} = 5.5$ s^{-1} $p_1 = 0.59$, $p_2 = 0.41$ (sites are labelled in this and later figures in accord with the labelling system used in Tables 1 and 2)

the low-field (A1) doublet was additionally broadened as compared with the high-field (B1) doublet, which was closer to the averaged chemical shift of A2 and B2 (see Figure 2 for an illustration). The exchange rates k_{12} and k_{21} are related by $p_1k_{12} = p_2k_{21}$ and for $p_2 \ll p_1$ a similar line-shape could be obtained either by the method outlined above or by treating the spectrum as a single coalescing AB system (A1 and B1) with the exchange rate $k = 0.5\ k_{12}$. However, this simplified treatment fails, for the reasons described above, as p_2 increases. This result is of general interest in that it demonstrates that the widely used treatment of spectral line-shapes for inverting ring systems [7] which ignores the presence of intermediate conformations with a low population, for example, the twist-boat conformations of cyclohexane, is in accord with the above computational results.

The n.m.r. spectra of the thiocin derivative (2a) were simulated in a rather similar manner, but in this case the low intensity signals (AB2 and CD2) of the boat conformation were just detectable (Figure 3) and spectral simulation was based upon both pairs of AB systems. Thus the systems A1,B1 and A2,B2 (Figure 3 and Table 1) shown by the thiocin derivative (2a) correspond to its C-5 and C-7 methylene group protons and the systems C1,D1 and C2,D2 correspond to its C-12 methylene protons.

[14] J. W. Cook, *J. Chem. Soc.*, 1930, 1091.

* We thank Dr. W. Deloughry for writing this program.

† In cases in which $k_2 \gg k_{12}$ the site exchanges B1 ⇌ A2 and A1 ⇌ B2 would give spectral line-shapes identical with those based upon A1 ⇌ A2 and B1 ⇌ B2.

The n.m.r. spectra of the azocine derivative (2c) at low temperatures also showed signals associated with the

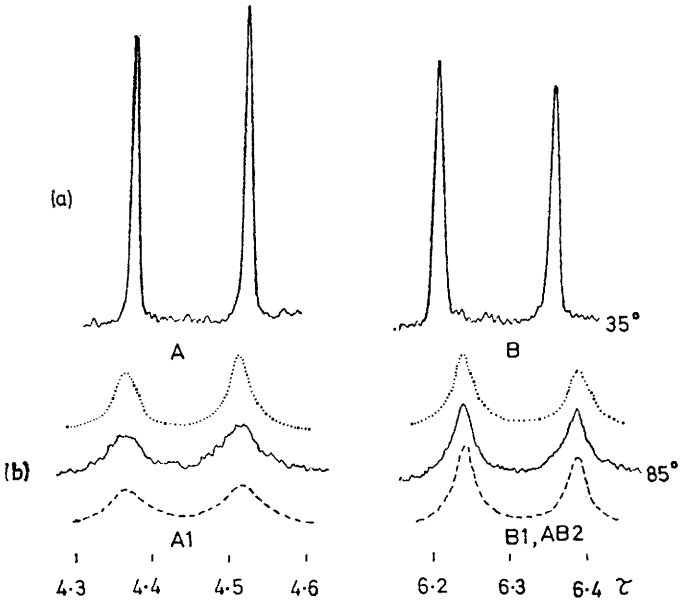

FIGURE 2 Observed (full line) and computed (broken line) spectra of the C-5 and C-7 methylene protons of the dithiocin derivative (2i): (a) at 35 °C, (b) at 85 °C; the broken line corresponds to the line-shape simulation by method I with $k_{12} = 6.5\ s^{-1}$, $p_1 = 0.95$, $p_2 = 0.05$, and the dotted line to the line-shape simulation by method III with $k = 13\ s^{-1}$

chair conformation (A1,B1 from the C-5 and C-7 methylene protons and C1,D1 from the C-12 methylene protons) and a rapidly inverting boat conformation (AB2 from the C-5 and C-7 methylene protons and CD2 from the C-12 methylene protons). Computed spectra were based upon C-5 and C-7 (A1,B1) methylene group protons. The program PLOTTER II [15] was used to generate theoretical line-shapes. This program sums the spectra of two AB systems, A1,B1 and C1,D1, with relative summed intensities 1.0 and 0.5 respectively and with exchange between the pairs of sites A1 and B1 and C1 and D1 with the same rate, k. This program could also be used to simulate the low temperature spectra of the compounds (2e and g) which both showed two AB systems of different intensities at low temperatures. The low intensity AB system (A2,B2) in both cases showed evidence, as the temperature

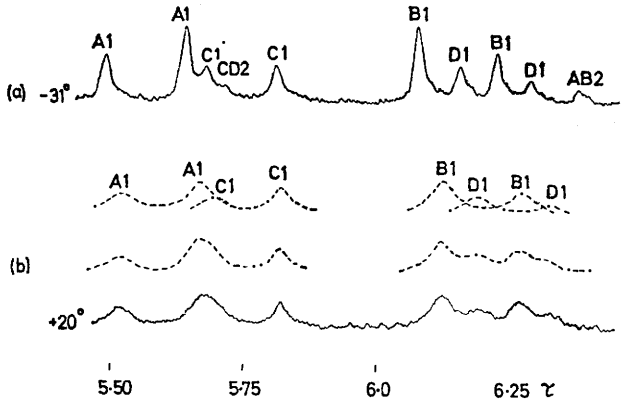

FIGURE 3 Observed (full line) and computed (broken line) spectra of the C-5, C-7, and C-12 methylene protons of the thiocin derivative (2a) at (a) −31 °C and (b) +20 °C; $k_{12} = 9.31\ s^{-1}$, $k_2 \longrightarrow \infty$ (method I), $p_1 = 0.91$, $p_2 = 0.09$; the upper computed spectrum shows the separate signals from the systems A1,B1, and C1,D1 and the lower the summed spectrum of these two systems

was raised, of mutual site exchange with a rate k_2 and gave the typical line-shapes [7] of a coalescing AB system. The

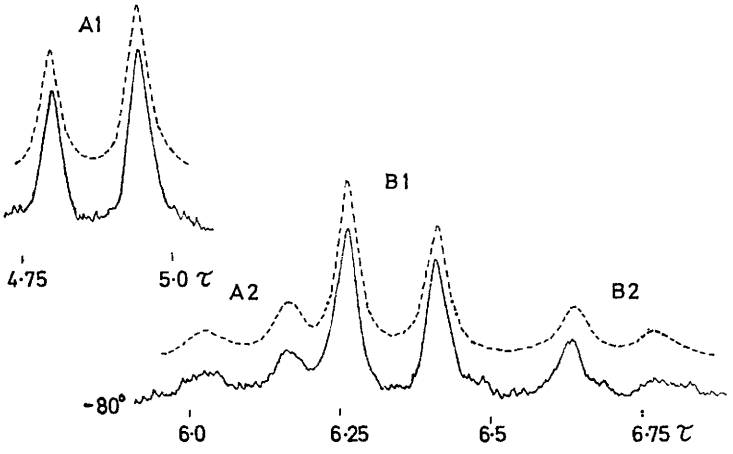

FIGURE 4 Observed (full line) and computed (broken line) spectra of the C-5 and C-7 methylene protons of the oxathiocin derivative (2e) at −88 °C, with $k_{12} = k_{21} = 0\ s^{-1}$ and $k_2 = 6.0\ s^{-1}$, $p_1 = 0.73$, $p_2 = 0.27$

these two pairs of AB systems as in the case of (2a). In addition, the *N*-benzyl methylene group of this azocine derivative (2c) gave two singlet signals corresponding to the chair and boat conformations; line-shapes in this case were simulated by method IV.

Method II. Compound (2b) gave, at low temperatures, two superimposed AB systems from the C-12 (C1,D1) and high intensity AB system (A1,B1) remained unchanged in this temperature range (k_1, k_{12}, and $k_{21} \longrightarrow 0$) and did not contribute to the line-shape changes of the system A2,B2. The use of this program is illustrated in Figures 4 and 5, which show the appearance of the observed and calculated spectra for compounds (2e and g) with $k_2 > 0$ and $k_{12} =$

[15] J. R. Fletcher, Ph.D. Thesis, Sheffield, 1970.

$k_{21} = 0$ and also the appearance of the spectrum as $k_2 \longrightarrow \infty$ and $k_{12} > 0$ [Figure 5(b)].

Method III. The disulphone (2j) gave only a single AB system at low temperature, and spectral line-shapes were

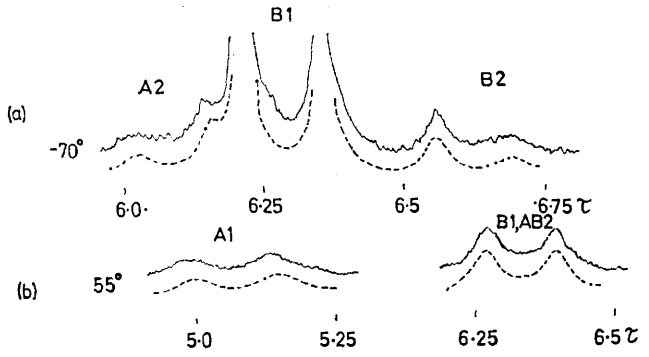

FIGURE 5 Observed (full line) and computed (broken line) spectra of the C-5 and C-7 methylene protons of the dithiocin derivative (2g): (a) at −70 °C, with $k_{12} = k_{21} = 0$, $k_2 = 8.05$ s^{-1}; (b) at +55 °C with $k_2 \longrightarrow \infty$, $k_{12} = 20.26$ s^{-1}, $p_1 = 0.81$, $p_2 = 0.19$

simulated using a program [15] PLOTTER I suitable for simulating the spectral line-shapes of a single AB system undergoing mutual site-exchange.

Method IV. The *N*-benzyl methylene group of compounds (2c, f, and h) gave two singlet signals of unequal intensities at low temperatures and spectral line-shapes were simulated using a program [16] NMREX 2 SITE suitable for exchange between two unequally populated sites with no mutual coupling. Exchange rates obtained using this program agreed well with those obtained from the line-shapes of the spectra of the C-5 and C-7 methylene group protons, confirming the general validity of the approach

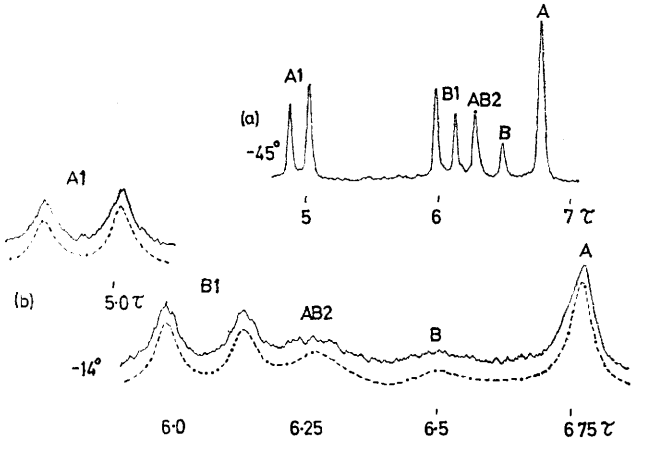

FIGURE 6 Observed (full line) and computed (broken line) spectra of the *N*-benzyl and C-5 and C-7 methylene protons of the thiazocine derivative (2h): (a) at −45 °C; (b) at −14 °C with $k_{12} = 9.28$ s^{-1}, $k_2 \longrightarrow \infty$ (method I) and $k_{AB} = 9.28$ s^{-1}, $p_A = 0.75$, $p_B = 0.25$ (method IV)

using method I. Calculated and observed spectra are shown in Figures 6 and 7 for compounds (2f and h).

Strain Energy Calculations.—These were carried out using a FORTRAN program based upon the procedure reported by Allinger *et al.*[17a] The program proved reasonably efficient, and the iterative procedure was continued until the root mean square atomic motion between successive iterations was consistently less than 0.001 Å in each co-ordinate. Free movement of all co-ordinates was allowed for minimum energy conformations, but for transition states appropriate atomic co-ordinates remained fixed throughout the minimisation procedure. Generally energy minimisation required 10—15 min computing time with an ICL 1907 computer. Many of the conformations examined involved large angle deformations, and it was clear from the results that force constants obtained from valence force field treatments for angle deformation are too large when large deformations are considered. All bending force constants were therefore reduced empirically by multiplication by 0.7 (*cf.* ref. 17). This modification of bending force constants has subsequently been found unnecessary for cases involving smaller angle deformation, and this agrees quite well with a modified expression for angle strain deformation which includes both quadratic and cubic terms.[17b] This difficulty in the correct calculation of strain energy resulting from angle deformation is a serious limitation of the calculations described in this paper.

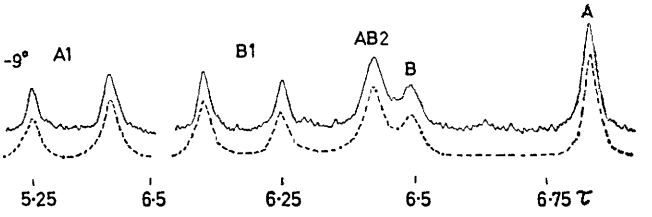

FIGURE 7 Observed (full line) and computed (broken line) spectrum of the *N*-benzyl and C-5 and C-7 methylene protons of the oxazocine derivative (2f) at −9 °C; $k_{12} = 3.80$ s^{-1}, $k_2 \longrightarrow \infty$ (method I) and $k_{AB} = 3.76$ s^{-1}, $p_A = 0.67$, $p_B = 0.33$

However, we feel that, although our results may lack quantitative significance, they are nevertheless of considerable help in understanding complex conformational changes.[18]

RESULTS AND DISCUSSION

The n.m.r. spectra of the heterocyclic analogues (2a—k) of 5,6,7,12-tetrahydrodibenzo[*a*,*d*]cyclo-octene in most cases showed temperature dependence associated with the presence of two conformational species in equilibrium, together with slow conformational inversion of one or both species. The spectral changes observed for the aromatic protons were complex and will not be discussed. The changes associated with the signals of the C-5 and C-7 methylene protons, and where relevant those of the C-12 and the *N*-benzyl methylene protons, are summarised in Tables 1 and 2. Table 1 summarises the chemical shifts and coupling constants of the high- and the low-temperature spectra. Table 2 gives details of site exchanges affecting the signal line-shapes, with associated rate constants and activation parameters. These are derived by comparison of observed and computed spectral line-shapes (see Figures 1—7) using methods I—IV (see Experimental section).

[15] I. R. Gault, Ph.D. Thesis, Sheffield, 1970.

[16] (*a*) N. L. Allinger, M. T. Tribble, M. A. Miller, and D. H. Wertz, *J. Amer. Chem. Soc.*, 1971, **93**, 1637; (*b*) E. M. Engler, J. D. Andose, and P. von R. Schleyer, *ibid.*, 1973, **95**, 8003.

[18] W. D. Ollis, J. F. Stoddart, and I. O. Sutherland, *Tetrahedron*, 1974, **30**, 1903.

TABLE 1

Temperature-dependent spectral parameters (100 MHz) for compounds (2a—l)

Compd.	X	Y	Solvent	Temp. (°C)	Group	N.m.r. parameters [a] [τ (coupling constant)]
(2a)	CH_2	S	$CDCl_3$	−31	$ArCH_2{\cdot}S$	5.58 (A1), 6.15 (B1) (*J* 15.0 Hz)
					$ArCH_2{\cdot}S$	6.39 (s) (AB2)
					$ArCH_2Ar$	5.76 (C1), 6.22 (D1) (*J*13.1 Hz)
					$ArCH_2Ar$	5.72 (s) (CD2)
(2b)	CH_2	SO_2	C_5D_5N	0	$ArCH_2{\cdot}SO_2$	4.09 (A1), 5.26 (B1)(*J* 14.5 Hz)
					$ArCH_2Ar$	5.27 (C1), 5.97 (D1) (*J* 13.0 Hz)
				95	$ArCH_2{\cdot}SO_2$	5.15 (s) (AB1)
					$ArCH_2Ar$	5.76 (s) (CD1)
(2c)	CH_2	$N{\cdot}CH_2Ph$	$CDCl_3$	−30	$ArCH_2{\cdot}N$	5.36 (A1), 5.98(B1) (*J* 15.0 Hz)
					$ArCH_2{\cdot}N$	6.26 (s) (AB2)
					$ArCH_2Ar$	5.50 (C1), 6.28 (D1) (*J* 12.9 Hz)
						5.56 (s) (CD2)
					$N{\cdot}CH_2Ph$	6.80 (s) (A)
					$N{\cdot}CH_2Ph$	6.19 (s) (B)
(2d)	O	S	$CDCl_3$	−57	$ArCH_2{\cdot}S$	5.64 (A1), 6.32 (B1) (*J* 14.7 Hz)
					$ArCH_2{\cdot}S$	6.49 (s) (AB2)
				40	$ArCH_2{\cdot}S$	6.27br (s) (AB12)
(2e)	O	SO_2	$CDCl_3$–CS_2 (2 : 1)	−88	$ArCH_2{\cdot}SO_2$	4.88 (A1), 5.83 (B1) (*J* 14.5 Hz), 5.60 (A2), 6.19 (B2) (*J* 13.9 Hz)
				−3	$ArCH_2SO_2$	5.68br (s) (AB12)
(2f)	O	$N{\cdot}CH_2Ph$	$CDCl_3$	−29	$ArCH_2{\cdot}N$	5.34 (A1), 6.17 (B1) (*J* 14.7 Hz), 6.43 (s) (AB2)
					$N{\cdot}CH_2Ph$	6.84 (s) (A), 6.50 (s) (B)
				40	$ArCH_2{\cdot}N$	6.2br (s) (AB12)
					$N{\cdot}CH_2Ph$	6.70 (s) (AB)
(2g)	S	S	CS_2	−85	$ArCH_2{\cdot}S$	5.11 (A1), 6.36 (B1) (*J* 14.2 Hz), 6.17 (A2), 6.70 (B2) (*J* 13.7 Hz)
			$CDCl_3$	20	$ArCH_2{\cdot}S$	5.06 (A1), 6.32 (B1) (*J* 14.2 Hz), 6.36 (s) (AB2)
(2h)	S	$N{\cdot}CH_2Ph$	$CDCl_3$	−45	$ArCH_2{\cdot}N$	4.96 (A1), 6.05 (B1) (*J* 14.5 Hz), 6.29 (s) (AB2)
					$N{\cdot}CH_2Ph$	6.78 (s) (A), 6.49 (s) (B)
				80	$ArCH_2N$	5.66 (s) (AB12)
					$N{\cdot}CH_2Ph$	6.67 (s) (AB)
(2i)	SO_2	S	$CDCl_3$	35	$ArCH_2{\cdot}S$	4.46 (A1), 6.28 (B1) (*J* 14.9 Hz) [6.50(AB2)] [b]
(2j)	SO_2	SO_2	$CDCl_3$	35	$ArCH_2{\cdot}SO_2$	3.77 (A1), 5.89(B1) (*J* 14.5 Hz)
(2k)	SO_2	$N{\cdot}CH_2Ph$	$CDCl_3$	35	$ArCH_2{\cdot}N$	4.46 (A1), 6.03 (B1) (*J* 15.0 Hz) [6.10 (AB2)] [b]
					$N{\cdot}CH_2Ph$	6.83 (s)
(2l)	CO	$N{\cdot}CH_2Ph$	$CDCl_3$	35	$ArCH_2{\cdot}N$	6.26 (s) (AB2) [c]
					$N{\cdot}CH_2Ph$	6.39 (s)

[a] The designations A1, B1, *etc.* correspond to the site exchanges cited in Table 2. The designations AB1, AB2 refer to coalesced signals from the AB systems A1,B1 or A2,B2 respectively. The designation AB12 refers to the single coalesced signal from the AB systems A1,B1 and A2,B2. The designation AB refers to the coalesced singlet signals A and B. [b] The square brackets indicate that this signal was inferred from line-shape calculations but was not visible in the spectrum above the noise level. [c] This signal is designated AB2 since it may be assigned to a rapidly inverting boat conformation.

An examination of molecular models, supported by strain energy calculations (see Experimental section and Tables 3 and 4), shows that the compounds (2) can adopt two types of conformation, both of which are almost free from angle strain. The first of these is the rigid chair-like conformation (4) which has C_s symmetry. The C-5 and C-7 methylene protons of this conformation, H^1 and H^2 [see structures (4)] are exchanged between the sites A1 and B1 by the conformational inversion (4a) ⇌ (4b); it is therefore necessary when discussing the n.m.r. results to consider these two identical conformations (4a and b) separately. They are designated C and C* in the discussion that follows. The conformations of the compounds (2), and the relationships between conformations, are also conveniently considered in the terms of the torsional angles associated with the single bonds of the eight-membered ring, and these are described using the conventional + and − notation,[1,19] illustrated in the Newman projections (5a—c). The signs of the torsional angles about the single bonds of the eight-membered ring of the compounds (2) are accordingly listed below each of the conformational

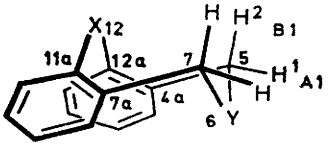

(4a) C (+ − + − + −)

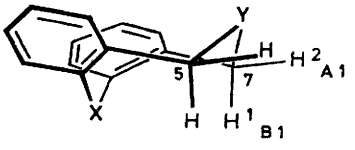

(4b) C* (− + − + − +)

(5a) + (5b) − (5c) 0

[19] W. Klyne and V. Prelog, *Experientia*, 1960, **16**, 521; J. B. Hendrickson, *J. Amer. Chem. Soc.*, 1962, **84**, 3355; 1964, **86**, 4854; 1967, **89**, 7047.

TABLE 2

Site exchanges and activation parameters for conformational changes of compounds (2a—l)

Compd.	X	Y	Solvent	Method	Site exchanges [a]	T/°C	k[b]/s^{-1}	$\Delta G^{\ddagger}$/kcal mol^{-1}	p_1	p_2	ΔG^{c}/kcal mol^{-1}	Process [b]	Comments
(2a)	CH_2	S	$CDCl_3$	I	A1 ⇌ A2,	20	9.3	15.8	0.91	0.09	1.35	C ⟶ Boat	Assumed
					B1 ⇌ B2,		4.65	16.2				C ⇌ C *	k(A2 ⇌ B2) ⟶ ∞,
					C1 ⇌ C2,								k (C2 ⇌ D2) ⟶ ∞
					D1 ⇌ D2								
(2b)	CH_2	SO_2	C_5D_5N	III	A1 ⇌ B1,	44	67	15.9				C ⇌ C *	$\Delta G^{\ddagger}$ 15.5 kcal mol^{-1} for
					C1 ⇌ D1								C ⟶ Boat
(2c)	CH_2	N·CH_2Ph	$CDCl_3$	I	A1 ⇌ A2,	49	19.2	17.0	0.93	0.07	1.34	C ⟶ Boat	Assumed
					B1 ⇌ B2		9.6	17.4			(−11°) [d]	C ⇌ C *	k(A2 ⇌ B2) ⟶ ∞,
					C1 ⇌ C2,		19.2	17.0	0.93	0.07		C ⟶ Boat	k (C2 ⇌ D2) ⟶ ∞
					D1 ⇌ D2								
				IV	A ⇌ B								
(2d)	O	S	$CDCl_3$	I	A1 ⇌ A2,	−26.5	5.5	13.5	0.59	0.41	0.18	C ⟶ Boat	Assumed
					B1 ⇌ B2								k(A2 ⇌ B2) ⟶ ∞
							2.75	13.8				C ⇌ C *	
(2e)	O	SO_2	$CDCl_3$–CS_2 (2 : 1)	I	A1 ⇌ A2,	−52	7.9	11.9	0.73	0.27	0.44	C ⟶ Boat	Assumed
					B1 ⇌ B2								k(A2 ⇌ B2) ⟶ ∞
							3.95	12.2				C ⇌ C *	
				III	A2 ⇌ B2	−88	6.0	10.0				Boat ⇌ Boat *	Assumed
													k(A1 ⇌ B1) ⟶ 0
(2f)	O	N·CH_2Ph	$CDCl_3$	I	A1 ⇌ A2,	−9	3.8	14.7	0.67	0.33	0.37	C ⟶ Boat	Assumed
					B1 ⇌ B2								k(A2 ⇌ B2) ⟶ ∞
							1.9	15.1				C ⇌ C *	
				IV	A ⇌ B	−9	3.8	14.7				C ⟶ Boat	
(2g)	S	S	$CDCl_3$	I	A1 ⇌ A2,	55	20.3	17.3	0.81	0.19	0.94	C ⟶ Boat	Assumed
					B1 ⇌ B2								k(A2 ⇌ B2) ⟶ ∞
							10.1	17.8				C ⇌ C *	
				III	A2 ⇌ B2	−70	8.1	10.9	0.89	0.11	0.84	Boat ⇌ Boat *	Assumed
													k(A1 ⇌ B1) ⟶ 0
(2h)	S	NCH_2Ph	$CDCl_3$	I	A1 ⇌ A2,	−14	9.3	13.9	0.75	0.25	0.57	C ⟶ Boat	Assumed
					B1 ⇌ B2								k(A2 ⇌ B2) ⟶ ∞
							4.6	14.3				C ⇌ C *	
				IV	A ⇌ B	−14	9.3	13.9				C ⟶ Boat	
(2i)	SO_2	S	$CDCl_3$	I	A1 ⇌ A2,	85	13.0	19.3	0.95	0.05	2.1	C ⟶ Boat	Assumed
					B1 ⇌ B2								k(A2 ⇌ B2) ⟶ ∞
							6.5	19.8				C ⇌ C *	p_2 obtained by line-shape comparison
(2j)	SO_2	SO_2	$CDCl_3$	II	A1 ⇌ B1	60	11.5	18.0	*ca.* 1.0	*ca.* 0.0		C ⇌ C *	$\Delta G^{\ddagger}$ 17.5 kcal mol^{-1} for
													C ⟶ Boat
(2k)	SO_2	N·CH_2Ph	$CDCl_3$	I	A1 ⇌ A2,	60	12.8	17.9	0.94	0.06	1.8	C ⟶ Boat	Assumed
					B1 ⇌ B2								k(A2 ⇌ B2) ⟶ ∞
							6.4	18.3				C ⇌ C *	p_2 obtained by line-shape comparison
(2l)	CO	N·CH_2Ph	$CDCl_3$		A2 ⇌ B2	−110	>132	<7.8	*ca.* 0.0	*ca.* 1.0	<−2.3	Boat ⇌ Boat *	Assuming ($\nu_A - \nu_B$) = 50 Hz and J_{AB} = 13 Hz

[a] Details of chemical shifts and coupling constants are given in Table 1. The AB systems A1,B1 and C1,D1 refer to the C-5, and C-7, and C-12 methylene protons of the chair (major conformation) and A2,B2 and C2,D2 to the boat (minor) conformation. [b] k(C ⟶ C*) = 0.5k(C ⟶ Boat) if the inversion process involves the intermediate boat conformation (see Figure 8), but if the two degenerate pathways, C ⟶ TB, are involved in the inversion then for a single C ⟶ TB process k(C ⟶ Boat) = k (C ⟶ C*). [c] At the temperature in column 7 unless otherwise stated. The value given refers to the process C ⟶ Boat. [d] From the spectrum in $CDCl_4$ at −11 °C.

diagrams † used in this paper in the order of bonds 4a,5, 5,6, 6,7, 7,7a, 11a,12, and 12,12a [numbering scheme shown in diagrams (2) and (4a)].

The second conformational type includes a family of boat-like conformations (Boat) ‡ and two pairs of these conformations may be distinguished on the basis of their symmetry. The first of these pairs comprises the conformations B and B* (6a and b) which have C_s symmetry. This symmetrical conformation can undergo changes which involve principally torsion about the 5,6- and 6,7-bonds to give eventually the second pair of symmetrical conformations TB and TB* (7a and b) which have C_2 symmetry (the C_2 axis is indicated by the broken line). This type of conformational behaviour has been discussed [6] for cyclo-octa-1,4-diene, and it has been pointed out that some angle deformation must be involved in the process analogous to B (6a) ⟶ TB (7a). The relative energies of the B and TB conformational types clearly depend upon the nature of the groups X and Y, and these energies have been calculated for the dibenzothiocin derivative (2a) (X = CH_2, Y = S) and the dibenzazocine derivative (2m) (X = CH_2, Y = NMe). These calculations (Tables 3 and 4) show that the C_s conformations B and B* (6a and b) involve, as expected, non-bonded interactions between the groups X and Y which result in considerable strain energy, although the interactions are substantially reduced by a flattening distortion of the eight-membered ring. These interactions are steadily reduced during the process B ⟶ TB, although the attainment of C_2 symmetry § in the TB and TB* conformations (7a and b) requires the introduction of some strain in the eight-membered ring

TABLE 3

Calculated strain energy [a,b] (E_S/kcal mol^{-1}) of various conformations of 7,12-dihydro-5*H*-dibenzo[*c*,*f*]thiocin (2a)

Conformation	$\phi_{5,6}$	$\phi_{6,7}$	E_S	E_R	E_θ	E_ϕ [c,d]	E_Δ [d]	E_{NBI} [e]	E_{NBIR} [e]
C	−88.2	+88.2	1.87	0.15	1.18	1.95	0.04	−1.45	3.19
B	+72.0	−71.9	9.67	0.35	7.70	0.48	0.12	1.03	5.19
TB	−59.0	−59.0	5.21	0.24	4.88	0.40	0.66	−0.97	3.29
Boat [g]	−22.9	−84.0	5.10	0.24	2.60	2.21	0.12	−0.07	4.11
Boat [f]	−27.5	−80.7	5.30	0.24	3.14	1.82	0.17	−0.05	4.11
Boat [f]	0	−97.7	5.37	0.22	1.61	3.55	0.02	−0.03	3.88
Boat [f]	+21.46	−109.1	5.61	0.25	1.13	3.53	0.07	0.63	4.23
Boat [f]	+41.38	−113.0	5.84	0.31	1.94	2.56	0.06	0.97	4.57
TS1 [h]	0	+60.0	19.43	0.56	16.70	2.14	0.16	−0.12	4.22
TS2 [h]	−112.1	+103.9	33.27	0.75	27.90	3.79	0.08	0.75	4.47
TS3 [h]	0	0	21.59	0.29	16.71	4.38	0.62	−0.41	3.39

[a] Calculations based upon the following force constants. Bond stretch: aromatic k_{CC} 1 102, k_{CH} 729; aliphatic k_{CC} 663, k_{CH} 655, k_{CS} 463 kcal Å^{-2}. Angle deformation: aromatic k_{CCC} 144, k_{CCH} 108; aliphatic k_{CCC} 115, k_{CCH} 94, k_{HCH} 79, k_{CSC} 100, k_{SCH} 89 kcal radian^{-2}, all angle strain reduced by a factor of 0.7. [b] Equilibrium bond lengths and bond angles assumed as follows: aromatic C–C 1.395, C–H 1.09; aliphatic Ar–C 1.50, C–S 1.80, C–H 1.09 Å; aromatic CĈC 120°, CĈH 120°; aliphatic CĈC 111.5°, CĈH 109.5°, HĈH 108°. [c] For C–S bonds a 3-fold barrier of height 2.1 kcal mol^{-1} is assumed. [d] For aromatic C–C bond twisting and out-of-plane deformation E_ϕ and E_Δ were calculated according to ref 18. [e] Non-bonded interactions based upon the Hill equation as summarised in ref. 16. [f] Boat conformations defined by torsion angles about 5,6- and 6,7-bonds, $\phi_{5,6}$ fixed by fixing appropriate atom co-ordinates. [g] Minimum energy boat conformation obtained by starting with $\phi_{5,6}$ −27.5° $\phi_{6,7}$ −86.1° and allowing free movement of co-ordinates. [h] TS1 defined by keeping atoms 12a, 4a, 5, 6, and 7 coplanar, TS2 by keeping atoms 4a, 7a, 11a, 12, and 12a coplanar, and TS3 by keeping atoms 4a, 5, 6, 7, and 7a coplanar.

TABLE 4

Calculated strain energy [a] (E_S/kcal mol^{-1}) of various conformations of 5,6,7,12-tetrahydro-6-methyldibenz[*c*,*f*]azocine (2; X = CH_2, Y = NMe)

Conformation	$\phi_{5,6}$	$\phi_{6,7}$	E_S	E_R	E_θ	E_ϕ	E_Δ	E_{NBI}	E_{NBIR}
C	−83.7	+83.7	4.30	0.16	1.92	3.99	0.10	−1.88	3.42
B	+83.0	−83.0	5.94	0.20	3.84	2.83	0.17	−1.10	4.22
TB	−58.4	−58.4	5.62	0.33	5.48	0.17	0.26	−0.61	4.13
Boat [b]	−57.8	−59.3	5.54	0.32	5.32	0.19	0.40	−0.69	4.07
Boat [c]	−38.5	−70.1	6.23	0.32	3.95	1.65	0.40	−0.10	4.97
TS1B(TS1A)	63.5	0.0	22.58	0.68	17.04	4.57	0.07	0.23	5.36
TS2	111	112	33.36	0.57	23.87	8.36	0.01	0.56	5.23
TS3	0	0	27.29	0.33	16.20	9.52	1.94	−0.69	4.02

[a] Calculations based on the force constants summarised below Table 3 with the following additions: k_{CN} 716 kcal Å^{-2}, k_{CCN} 130, k_{CNC} 144, k_{CNH} 100 kcal radian^{-2}, angle strain reduced by a factor of 0.7. For CNC bonds a barrier height of 4.4 kcal mol^{-1} is assumed. Equilibrium bond lengths and bond angles as below Table 3 with the following additions: C–N 1.472 Å, CĈN 111.5°, NĈH 109.5°, CN̂C 109°. [b] From a TB starting conformation with retention of *C*2 symmetry of the 6-8-6 ring system and allowing loss of C_2 symmetry. [c] From a starting conformation with $\phi_{5,6}$ − 30.8, $\phi_{6,7}$ − 81.4.

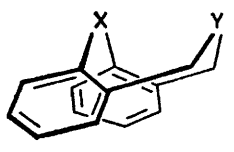

(6a) B (+ + − − + −)

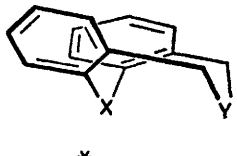

(6b) B* (− − + + − +)

† Conformational diagrams (4) and (6)—(8) are based upon computer-produced perspective drawings of the various energy-minimised conformations of the thiocin derivative (2a) (Table 3).

‡ In accord with the nomenclature used in our previous paper [1] the description 'Boat' refers to any conformation of the boat family. The descriptions B, B*, TB, and TB* are specific.

§ The conformational types TB and TB* (7a and b) do not have C_2 symmetry for Y = NR. This conformation, however, does have C_2 symmetry if the substituent on the nitrogen atom is ignored.

in addition to slight out-of-plane deformation of the aromatic rings (see Tables 3 and 4).

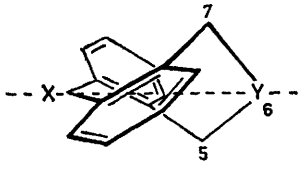

(7a) TB* (− + + − + +)

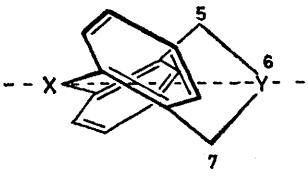

(7b) TB (+ − − + − −)

The torsional situations about the 5,6-and 6,7-bonds in the TB and TB* conformations (7) are close to ideal (torsion angles $\phi_{5,6}$ and $\phi_{6,7}$ close to 60°). In some cases torsional strain in the flattened B and B* conformations (6) may be small [*e.g.* for the thiocin derivative (2a)] whereas in other cases it may be appreciable [*e.g.* for the azocine derivative (2m)]. Although in both the cases examined by strain energy calculations the TB conformation (7) is less strained than the B conformation (6), the differences in strain energies vary and are clearly dependent upon the nature of the groups X and Y. The minimum energy boat conformation [see (8)] for the thiocin derivative (2a) lies fairly close to the TB conformation [see (7)]. However the situation is less clear for the azocine derivative (2m) and there is apparently little difference in energy between the various Boat conformations that lie on the pathway TB ⟶ B ⟶ TB* ⟶ B*. From general considerations it is probable that for most of the compounds (2), the minimum energy Boat conformation lies rather closer to TB (7) than to B (6). In cases where the group X can conjugate with the aromatic rings then the TB conformation will be additionally favoured by the relatively small torsion angles about the 11a,12- and 12,12a-bonds [see (7)].

Having considered possible minimum energy conformations for the compounds (2), we must now consider pathways by which these conformations may be interconverted, and possible transition states for each pathway. These have been examined by strain energy calculations for the thiocin derivative (2a) (Table 3) and the azocine derivative (2m) (Table 4). The following generalisations are based upon these calculations and an examination of molecular models.

The low energy boat conformations TB and TB* (7) are interconverted, by a process involving principally torsion about the single bonds of the eight-membered ring analogous to the pseudo-rotation of the boat conformations of six-membered rings, by way of the conformations B and B* (6). On the basis of the results presented in Tables 3 and 4, this process will generally involve relatively low energy barriers: conformations showing the spectral characteristics of rapid inversion are therefore assigned as Boat.

The diastereoisomeric C and Boat conformations are interconvertible by three definable pathways involving three different transition states, TS1, TS2, and TS3. The transition state TS1 (9) lies on the pathway C ⟶ TB and is defined by the coplanarity of atoms 12a, 4a, 5, 6, and 7 [TS1A, (9a)] or atoms 11a, 7a, 7, 6, and 5 [TS1B, (9c)]. These chiral conformations are related as mirror images, but it is convenient when discussing spectral changes to consider additionally the conformations TS1A* (9b) and TS1B* (9d), and the distinction between these four conformational types is recognisable by the numbering scheme used in formulae (9) to indicate coplanarity of sets of atoms. Calculations indicate (Tables 3 and 4) that the principal source of strain in these conformations TS1 (9) is angle deformation (E_θ), and that in addition torsional strain is associated with the eclipsed 5,6- (TS1A) or 6,7-bond (TS1B). The second type of transition state TS2 (10) has C_s symmetry and lies on the pathways B ⇌ C* and B* ⇌ C; it is defined by the coplanarity of atoms

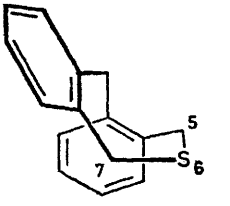

(8a) Boat (+ − − + + −)
$\phi_{5,6}$ −22·9
$\phi_{6,7}$ −84·0

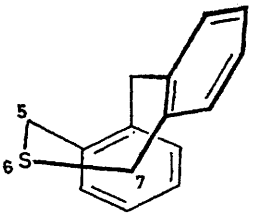

(8b) Boat* (− + + − − +)
$\phi_{5,6}$ +22·9
$\phi_{6,7}$ +84·0

4a, 7a, 11a, 12, and 12a. This transition state involves considerable angle deformation in addition to torsional strain, and is, in the two cases examined by strain energy calculations, significantly higher in energy than the other two transition states. The third transition state TS3 (11) also has C_s symmetry and lies on the pathways B ⇌ C and B* ⇌ C*. It is defined by the coplanarity of atoms 4a, 5, 6, 7, and 7a and although it involves angle strain rather similar in magnitude to the transition state TS1 (9), it is higher in energy owing to the additional torsional strain associated with eclipsed 5,6- and 6,7-bonds.

The relationships amongst the conformational types C, B, TB, TS1, TS2, and TS3 are summarised in Figure 8. It is now necessary to relate this scheme to the n.m.r. spectra, and their temperature dependence for compounds (2a—l), summarised in Tables 1 and 2.

On the basis of the information in Tables 1 and 2 compounds (2a—k) can be grouped according to three main types (1—3) of spectral temperature dependence. The relationships between the rate constants for the

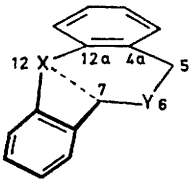

(9a) TS1A (0 0 + − + −)

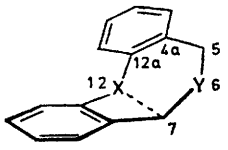

(9b) TS1A* (0 0 − + − +)

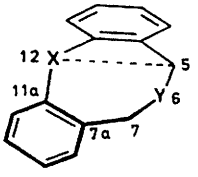

(9c) TS1B (+ − 0 0 + −)

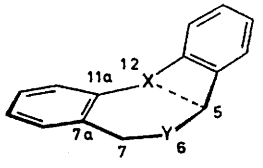

(9d) TS1B* (− + 0 0 − +)

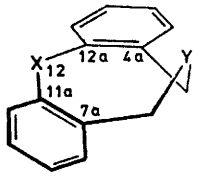

(10a) TS2 (− + − + 0 0)

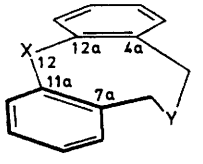

(10b) TS2* (+ − + − 0 0)

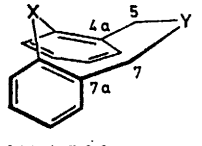

(11a) TS3

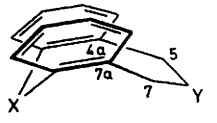

(11b) TS3*

conformational changes, summarised in Figure 8, and the site-exchange rates, deduced from spectral line-shapes (see Experimental section and below), are summarised in Figure 9.

Type 1. The spectra of the C-5 and C-7 methylene protons of compounds of this type (2b, i, j, and k) appear to consist of just a single AB system at low temperatures (sites A1 and B1, Figure 9) which coalesces to a singlet at higher temperatures. The spectra in some cases show some asymmetry for site exchange rates at which some line-broadening occurs (Figure 2), but below the exchange rate at which the A and B signals coalesce. For compounds (2i and k) this asymmetrical line shape can be reproduced using method I by inserting into the calculation a few percent of a rapidly inverting boat conformation (Figure 9; $k_2 \longrightarrow \infty$; see also Experimental section). On the other hand, for the remaining two compounds of this type (2b and j) a reasonably good agreement between computed and observed spectra could be obtained using methods II and III (Experimental section) without postulating additional site exchanges involving the Boat conformation. The additional temperature dependence of the C-12 methylene protons of the monosulphone (2b) was included in the simulated spectra by using method II.

Type 2. These compounds (2a, c, d, f, and h) show a singlet signal (AB2) in their n.m.r. spectra at low temperatures which is assignable to the C-5 and C-7 methylene groups of a rapidly-inverting, mobile conformation which must be of the Boat type. In addition the spectra show an AB system (A1,B1) associated with the C-5 and C-7 methylene groups of a slowly inverting conformation which must be of the Chair type. These assignments of signals to Chair and Boat conformations follow directly from the discussion of low energy conformational species and the strain energy calculations listed in Tables 3 and 4. Spectral line-shapes for these compounds can be accurately reproduced (Figures 1, 3, 6, and 7) using method I for the line-shape calculations together with a fast input rate for the inversion of the Boat conformation (Figure 9; $k_2 \longrightarrow \infty$). Under these conditions the spectral line-shapes depend, as expected, only upon the average chemical shift of the A2 and B2 sites and the population, p_2, of the Boat conformation. The separate chemical shifts of the A2 and B2 sites and the coupling constant J_2, which are not obtainable from the low temperature spectra, are not required for line-shape computation. The rate for the process C $\longrightarrow$ Boat (Figure 9; k_{12}) is twice the rate for the transformation C $\longrightarrow$ C* (see Figure 9): the rates and free energies of activation are given in Table 2 for both processes. As the population of the Boat conformation, p_2, tends to zero, the spectral line-shapes tend to those of

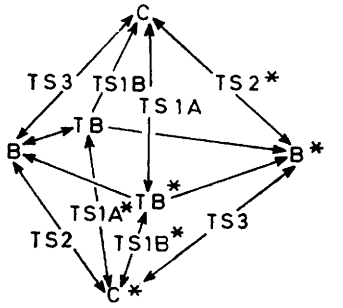

FIGURE 8 Conformational changes of heterocyclic analogues (2) of 5,6,11,12-tetrahydrodibenzo[*a*,*d*]cyclo-octene

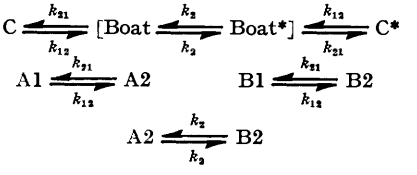

FIGURE 9 Relationships between rate constants for conformational changes and rate constants used for computation of spectral line-shapes.

a single coalescing AB system, with sites A1 and B1, coupling constant J_1, and site exchange rate $k_1 = 0.5\ k_{12}$ (see Figure 2). This latter situation resembles that found most frequently for ring-inversion processes.

For the amines (2c, f, and h), the n.m.r. spectra show two singlet signals at low temperature assignable to the *N*-benzyl methylene groups of Chair and Boat conformations. These coalesce to a single singlet at higher temperatures and line-shapes for this region of the n.m.r. spectrum may be accurately simulated using method IV. The close agreement of rate constants for these three compounds obtained by methods I and IV (Figures 6 and 7) confirms the general correctness of the approach used for line-shape simulation by method I.

Type 3. These two compounds (2e and g) give n.m.r. spectra for the C-5 and C-7 methylene protons that are similar to those of compounds of type 2, but at low temperatures the rate of inversion of the Boat conformation is sufficiently slow for a second low intensity AB system (A2,B2) to be observed. For these cases the rate of inversion of the boat conformation (Figure 9; k_2) may be obtained from low temperature spectral line-shapes using method I for spectrum simulation [with input values of $k_{12} = k_{21} = 0$ as in Figures 4 and 5(a)]. For spectra recorded at higher temperatures the rate constants, k_{12} and k_{21}, associated with the process Chair $\rightleftharpoons$ Boat may be obtained using method I as for compounds of type 2 [Figure 5(b)].

Rates of Conformational Change and Activation Parameters.—The rates of conformational change for compounds (2a—k) were measured by matching observed and computed spectral line-shapes at a single selected temperature (Table 2 and Figures 1—7). The discussion that follows is based upon the premise that for a conformational change the entropy of activation, $\Delta S^{\ddagger}$, is near zero. The potential energy difference between the minimum energy conformation and the transition state for a conformational change is therefore best compared with the free energy of activation for the change, $\Delta G^{\ddagger}$. The free energies of activation for the process C $\longrightarrow$ Boat for compounds (2a—k) are listed in Table 2, which in addition lists free energies of activation for the process C $\rightleftharpoons$ C*, since in some cases this is the only observable process. If the process C $\longrightarrow$ Boat involves the chiral transition states TS1A (9a) and TS1B (9c) [and similarly C* $\longrightarrow$ Boat* involves TS1A* (9b) and TS1B* (9d)], there are two equivalent pathways available for the transformation. Therefore the observed free energy of activation must be corrected by the addition of $RT\ln 2$ before being compared with the calculated potential energy of activation (see scheme in Figure 8). On the other hand, if the transition state for the process C $\longrightarrow$ Boat is actually the achiral conformation TS3 (11), only a single pathway is available and the correction should not be applied. On the basis of the strain energy calculations reported in Tables 3 and 4, it is doubtful whether the pathways C $\longrightarrow$ Boat* and C* $\longrightarrow$ Boat, involving the achiral transition states TS2 and TS2* (10), contribute to any of the observable conformational changes of compounds (2a—k).

Comparison of the data in Tables 3 and 4 with those in Table 2 for the thiocin derivative (2a) ($\Delta G^{\ddagger}$ 16.2 kcal mol^{-1} for C $\longrightarrow$ Boat, corrected for a single pathway involving TS1, and $\Delta E^{\ddagger}$ 17.6 kcal mol^{-1} based upon the strain energy difference between the conformations C and TS1) shows that the best agreement is obtained between observed and calculated energies of activation if the conformation TS1 (9) is the rate-determining transition state. Similarly an assignment of transition state geometry to the conformation TS1 (9) also leads to best agreement between observed and calculated activation energies for the azocine derivatives (2; X = CH_2, Y = NMe or N·CH_2Ph) ($\Delta G^{\ddagger}$ 17.4 kcal mol^{-1} for C $\longrightarrow$ Boat, corrected for a single pathway involving TS1, and $\Delta E^{\ddagger}$ 18.2 kcal mol^{-1} based upon the strain energy difference between conformations C and TS1).

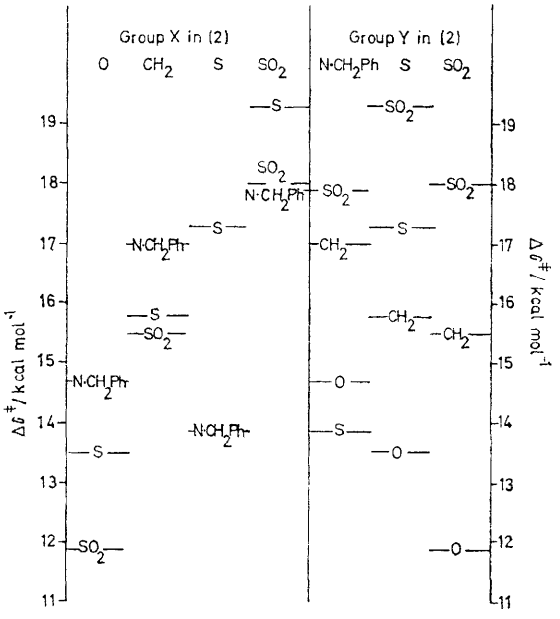

FIGURE 10 Relationships between $\Delta G^{\ddagger}$ (C $\longrightarrow$ B) and groups X and Y [see (2)]. The horizontal lines are placed correctly on a vertical energy scale, each line representing the value of $\Delta G^{\ddagger}$ for the single compound having the group Y or X indicated on the line. The left hand set refers to the group X remaining constant and Y changing, and the right hand set to group Y remaining constant and X changing

These results suggest that similar pathways involving the transition state TS1 (9) are followed for the conformational change, C $\longrightarrow$ Boat, for all the compounds (2a—k). The relative free energies of activation should therefore be related to the relative strain energies of the conformations C (4) and TS1 (9). Unfortunately strain energy calculations cannot be made with confidence for compounds (2; X = O, S, or SO_2) in which the aromatic rings are potentially conjugated with a heteroatom in position 12, owing to the difficulties associated with the selection of potential functions for deformation of the Ar–X–Ar fragment. The discussion that follows is therefore necessarily qualitative.

The relative heights of the free energy barrier for the process C $\longrightarrow$ Boat are shown in Figure 10, which illustrates the effects of a change in the groups X and Y upon the energy barrier. From the strain energy

calculations in Tables 3 and 4, these activation energies reflect principally angle strain in the eight-membered ring of TS1 (9) and an increase in non-bonded interactions in TS1. The increase in angle strain is associated principally with the angles α, β, γ, and δ of the eight-membered ring [see (12)], which are opened up to values in TS1 considerably greater than

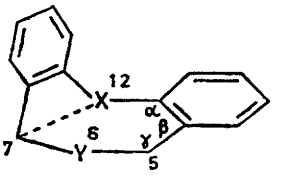

(12)

equilibrium values. The changes in non-bonded interactions are principally associated with a marked increase in the interaction between $C(12)H_2$ and $C(7)H_2$ in the conformation TS1 [see (12)] relative to C and a rather smaller decrease in the interaction between $C(12)H_2$ and $C(5)H_2$. In addition, for azocine derivatives (12; X = NR), non-bonded interactions involving the substituent on the nitrogen atom are also increased in TS1.

In view of the dominant part played by angle strain in determining the relative energies of the C and TS1 conformations, and hence the relative rates of the process C ⟶ Boat for the compounds (2a—k), a series of approximate calculations of angle strain in TS1 (9) was carried out. The results are summarised in Table 5.

TABLE 5

Calculated [a] and observed values of $\Delta G^{\ddagger}$ for the process C ⟶ Boat for compounds (2a, c, d, f, g, and h)

Compound	X	Y	Bond lengths (Å) Ar–X	CH_2–Y	E_θ in TS1 /kcal mol^{-1}	$\Delta G^{\ddagger}$ (C ⟶ B) /kcal mol^{-1}
(2a)	CH_2	S	1.51	1.82	14.2	15.8
(2c)	CH_2	NR	1.51	1.47	16.0	17.0
(2d)	O	S	1.42	1.82	13.2	13.5
(2f)	O	NR	1.42	1.47	15.3	14.7
(2g)	S	S	1.76	1.82	16.4	17.3
(2h)	S	NR	1.76	1.47	17.3	13.9

[a] Based upon the angle strain E_θ in TS1 [see (9) and (14)] using the expression $E_\theta = 0.021914\ (2\Delta\varepsilon^2 + \Delta\alpha^2 + \Delta\beta^2 + \Delta\gamma^2 + \Delta\delta^2)$ kcal mol^{-1}, where Δε, *etc.* are the deviations from the unstrained values: $\alpha = \beta = \varepsilon = 120°$, $\gamma = 111°$, and $\delta = 109°$ [see (14)]. For all compounds the unstrained values for the bond lengths d_1 and d_2 [see (14)] are taken as 1.39 Å (d_1) and 1.51 Å (d_2).

In view of the uncertainty regarding relative values of force constants for angle deformation, the same force constant was used for all the angles considered in the calculations, as in our earlier work [1] on heterocyclic analogues of 5,6,11,12-tetrahydrodibenzo[*a*,*e*]cyclooctene (1). The value of approximate calculations of this type is strictly limited. However, the results do show that the differences in the energies of activation for the process C ⟶ Boat are consistent with changes in angle strain in the transition states TS1. The origin of these differences lies in the changes in the lengths of the Ar–X and C–Y bonds; the activation energies increase with increasing Ar–X and decrease with increasing C–Y bond length (Table 5).

The observed higher free energies of activation for the sulphones (2; X = SO_2) as compared with the sulphides (2; X = S) are also consistent with the transition state TS1 (9) for the process C ⟶ Boat. Thus there are important non-bonded interactions between one of the sulphone oxygen atoms and $C(7)H_2$ in TS1A (9a) [or $C(5)H_2$ in TS1B (9c)] which would be considerably increased relative to the corresponding interactions in the C conformation (4). On the other hand, the sulphones (2; Y = SO_2) show lower free energies of activation than the sulphides (2; Y = S); this presumably results from the different force constants and equilibrium values for angles and bond lengths associated with the groups CSO_2C and CSC, but insufficient is known about these parameters for detailed comment.

The experimental result for compound (2h) [$\Delta G^{\ddagger}$ (C ⟶ Boat) 13.9 kcal mol^{-1}] does not correlate at all well with the energy of activation derived from crude angle strain calculations (Table 5; calculated angle strain in TS1 17.3 kcal mol^{-1}). This lack of agreement may simply result from the very approximate nature of the calculations. However, in view of the rather good correlation for the other compounds listed in Table 5, it may indicate in this case that the geometry of TS1 (9) is not a good model for the transition state for the conformational change C ⟶ Boat.

The relative free energies of C and Boat conformations are difficult to discuss in a general way. Qualitatively it is evident from the data in Table 2 that ΔG (C ⟶ Boat) increases as the size of the group Y increases (Y = SO_2 > S > N·CH_2Ph). This is readily understandable in terms of the non-bonded interactions between X and Y in the conformation B (6), but these are present to an increasingly smaller extent in Boat conformations lying between B and TB and they disappear in the TB conformations (7). It is similarly difficult to discuss the energy barriers for the process Boat ⇌ Boat*, although on the basis of the strain energy calculations presented in Tables 3 and 4 it is probable that the transition state for this process is close to the B or B* conformation (6). We note that this process is slow, on the n.m.r. time scale, for only two of the compounds studied (2e and g), even at −110 °C, although in two other cases (2d and h) the signals assignable to the C-5 and C-7 methylene groups of the Boat conformation are considerably broadened at −110 °C and the associated free energies of activation may not be much less than 8—9 kcal mol^{-1}.

The amino-ketone (2l) is of particular interest in view of the suggestion,[20] made on the basis of indirect evidence, that the >CO,>NR transannular interaction is attractive rather than repulsive in certain medium-sized rings. The n.m.r. spectrum of (2l), in contrast with those of (2a—k), shows no temperature dependence down to

[20] F. A. L. Anet, A. S. Bailey, and R. Robinson, *Chem. and Ind.*, 1953, 944; N. J. Leonard, D. F. Morrow, and M. T. Rogers, *J. Amer. Chem. Soc.*, 1957, **79**, 5476; N. J. Leonard, T. L. Brown, and T. W. Milligan, *ibid.*, 1959, **81**, 504.

−110 °C. The two singlet signals assignable to the C-5 and C-7 methylene groups (τ 6.26) and the *N*-benzyl methylene group (τ 6.39) of (2l) have chemical shifts which are similar to those of the rapidly inverting Boat conformations of (2c) (τ 6.26 and 6.19), (2f) (τ 6.43 and 6.50), and (2h) (τ 6.29 and 6.49), which are rather different from the averaged chemical shifts for the C-5 and C-7 methylene protons and the *N*-benzyl methylene protons of the Chair conformation of these compounds [(2c): τ 5.67, 6.80; (2f): τ 5.75, 6.84; (2h): τ 5.50, 6.78]. It is therefore concluded that the amino-ketone (2l) adopts the Boat conformation, and from the lack of temperature dependence in its n.m.r. spectrum there appears to be less than 2—3% of the Chair conformation. The latter might well be undetectable owing to its low concentration, but assuming that the Chair ⟶ Boat exchange rate (k_{12}) would change from slow to fast in the temperature range over which the n.m.r. spectrum remains unchanged [−110 to +100 °C, *cf.* compounds (2c, f, and h)], this lack of observable line-shape changes sets a low value for the population of the Chair conformation.

The Boat conformation of compound (2l) [with ΔG (C ⟶ Boat) < −2.3 kcal mol^{-1} at 25 °C assuming <2% of the Chair conformation] suggests that the >CO,>NR interaction may be attractive to the extent of at least 2—3 kcal mol^{-1} [*cf.* compound (2f), having ΔG (C ⟶ Boat) 0.37 kcal mol^{-1}] as compared with the expected non-bonded interaction between the nitrogen and carbon atoms. The free energy of activation for the process B ⟶ B* for (2l) is evidently less than 8 kcal mol^{-1} from the lack of signal separation at low temperatures; assuming that the N,CO attractive interaction would be lost in the transition state for conformational inversion, and assuming that the free energy of activation for this process would otherwise be zero, an upper limit of *ca.* 8 kcal mol^{-1} is suggested for any attractive interaction that may be present. This range of 2—8 kcal mol^{-1} implies a weakly bonding interaction which may be represented in MO terms as involving four electrons in two of the three MOs resulting from linear combinations of the carbon and oxygen 2*p* orbitals together with a nitrogen sp^3 orbital in a homo-amide grouping with the bonding depicted in (13); the C,N distance in the undistorted C_s Boat (B) conformation shown in (13) would be *ca.* 2.4 Å but we have no

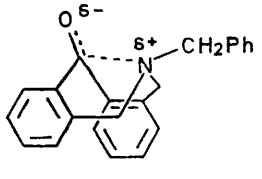

(13)

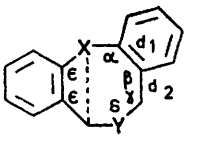

(14)

definitive information regarding the type of boat conformation actually adopted by the azocine derivative (2l).

Conclusions.—Compounds (2a—k) exist in Chair (4) and Boat conformations in solution, and in all the cases examined the Chair conformation is of lower energy. The kinetics of the process Chair ⟶ Boat may be determined by n.m.r. line-shape methods, and the associated activation parameters may be compared with the results of strain energy calculations. This comparison shows that the conformation TS1 (9) is the minimum energy transition state for this conformational change, and from the strain energy calculations (Tables 3 and 4) it is also evident that the energy barrier for the process Chair ⟶ Boat results principally from the considerable angle strain in the transition state TS1 (9). The conformational changes of compounds (2a—k) therefore provide a useful probe into the magnitude of angle strain for quite large angle deformations. In addition, for systems lacking ArXAr conjugation (X = CH_2), the measured activation energies for the process Chair ⟶ Boat may be used to examine various procedures to calculate angle strain.

The examination of compounds such as (2l) should provide information concerning the magnitudes of transannular interactions between >C=O and >NR groups which have previously been discussed [20] only in qualitative terms. These interactions have also been discussed for 1,8-bridged naphthalene derivatives.[18]

Pala *et al.*[11] have discussed briefly the n.m.r. spectrum of the azocine derivative (2c) and closely related compounds. The results agree essentially with ours although exchange rates and activation parameters were not reported. The dibenzazocine derivative (2m) has been examined in some detail and the results were published [21] after the completion of our studies.[18] The calculated values of ΔG and $\Delta G^{\ddagger}$ for Chair ⟶ Boat (' crown ' ⟶ ' flexible ' in the nomenclature of ref. 21) agree well with those determined in this work for the dibenzazocine derivative (2c), and are also in good agreement with the strain energy calculations for (2m) reported here [ΔG (Chair ⟶ Boat) 1.8 kcal mol^{-1}, $\Delta G_{211}^{\ddagger}$ (Boat ⟶ Chair) 15.3 kcal mol^{-1}, ΔH (Chair ⟶ Boat) 3.2 kcal mol^{-1}, ΔS (Chair ⟶ Boat) 7 ± 3 cal mol^{-1} K^{-1}, calculated ΔE (Chair ⟶ Boat) 1.24 kcal mol^{-1}, ΔE (Boat ⟶ TS1) 17.04 kcal mol^{-1}]. An examination [22] of the crystal structure of this dibenzazocine derivative (2m) has also been reported; the structure of the chair conformation found in the crystalline state is in reasonably good agreement with the structure details obtained from strain energy calculations. The corresponding *N*-t-butyl derivative (2n) is, however, found to adopt a boat conformation in the crystalline state,[23] and in solution, with torsion angles in the crystal midway between the conformations described in this paper as B (6) and TB (7) ($\phi_{5,6}$ −115.5°, $\phi_{6,7}$ +44.1° in one enantiomer and $\phi_{5,6}$ −64.5, $\phi_{6,7}$ +135.9 in the other).

[4/2699 *Received*, 30*th December*, 1974]

[21] R. N. Renaud, R. B. Layton, and R. R. Fraser, *Canad. J. Chem.*, 1973, **51**, 3380.

[22] A. D. Hardy and F. R. Ahmed, *Acta Cryst.*, 1974, **B30**, 1670.

[23] A. D. Hardy and F. R. Ahmed, *Acta Cryst.*, 1974, **B30**, 1674.